JACS
JOURNAL OF THE AMERICAN CHEMICAL SOCIETY

ARTICLE

pubs.acs.org/JACS

Persistence of the Three-State Description of Mixed Valency at the Localized-to-Delocalized Transition

Starla D. Glover and Clifford P. Kubiak*

Department of Chemistry and Biochemistry, University of California, San Diego, 9500 Gilman Drive MC 0358, La Jolla, California 92093, United States

Supporting Information

ABSTRACT: Application of a semiclassical three-state model of mixed valency to complexes of the type $[Ru_3(\mu_3\text{-}O)(OAc)_6(CO)(py)-(\mu_2\text{-}BL)-Ru_3(\mu_3\text{-}O)(OAc)_6(CO)(py)]^{-1}$, where BL = 1,4-pyrazine or 4,4′-bipyridine and py = 4-dimethylaminopyridine, pyridine, or 4-cyanopyridine is described. The appearance of two intervalence charge transfer (IVCT) bands in the near-infrared (NIR) region of the electronic spectra of these complexes is explained well by the three-state model. An important feature of the three-state model is that the IVCT band evolves into two bands: one that is metal-to-bridging-ligand-charge-transfer (MBCT) in character and another that is metal-to-metal-charge-transfer (MMCT) in character. The three-state model also fully captures the observed spectroscopic behavior in which the MBCT transition increases in energy and the MMCT band decreases in energy with increasing electronic communication in a series of mixed valence ions. The appearance of both the MBCT and MMCT bands is found to persist as coalescence of infrared (IR) vibrational spectra suggest a ground state delocalized on the picosecond time scale. The solvent and temperature dependence of the MBCT and MMCT electronic transitions defines the mixed valence complexes reported here as lying on the borderline of delocalization.

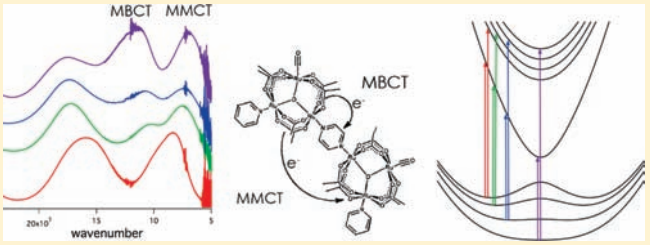

INTRODUCTION

The study of mixed valence complexes has been of interest to the chemistry, biology, and physics scientific communities for nearly 50 years.[1−3] The classifications of mixed valence complexes, originally defined by Robin and Day,[3] as class I (uncoupled), class II (moderately coupled), and class III (delocalized) have been applied to many systems, and these descriptions have been tested and refined by a variety of experimental methods.[4−12] One area that is still under discussion is the physical description and classification of complexes that lie somewhere along the border between class II and class III, at the threshold of delocalization.[13−15] Here, we describe the spectroscopic behavior of such borderline class II/III systems[16] in the case of the dimers of trinuclear ruthenium complexes, $[Ru_3(\mu_3\text{-}O)(OAc)_6(CO)(py)-(\mu_2\text{-}BL)-Ru_3(\mu_3\text{-}O)(OAc)_6(CO)(py)]^{-1}$, where BL = 1,4-pyrazine or 4,4′-bipyridine and py = 4-dimethylaminopyridine (dmap), pyridine (py), or 4-cyanopyridine (cpy) (**1**−**4**), Figure 1a. The range of electronic structures available in the series of mixed valence complexes $\mathbf{1}^-$−$\mathbf{4}^-$ affords an opportunity to examine several discrete points along the localized-to-delocalized transition. Previous work in our laboratories has established that the degree of electronic communication in mixed valence ions $\mathbf{1}^-$−$\mathbf{4}^-$ is controlled by the overlap between the d-orbitals of the Ru_3 clusters and the bridging pyrazine or bipyrdine π^* orbitals.[17] In pyrazine-bridged systems, more electron-donating ancillary pyridine ligands (i.e., dmap > py > cpy) raise cluster d-orbital energies relative to the pyrazine π^* orbital. This improved energetic alignment enhances electronic communication between Ru_3O units, Figure 1b. A particularly valuable characteristic of the mixed valence ions $\mathbf{1}^-$−$\mathbf{4}^-$ is that the rates of intramolecular electron transfer (ET) can be estimated from the degree of coalescence of the IR spectra of the carbonyl ligands in the ν(CO) region.[18,19] Figure 1c shows the ν(CO) spectra of $\mathbf{1}^-$−$\mathbf{4}^-$, and rate constants for ET, k_{ET}, estimated by simulation of the IR line shape.[19] Rate constants increase from ca. 4×10^{11} s^{-1} ($\mathbf{4}^-$) to ca. 3×10^{12} s^{-1} ($\mathbf{1}^-$) as the degree of electronic communication increases.

The assignment of mixed valence ions $\mathbf{1}^-$−$\mathbf{4}^-$ as "borderline class II/III"[6] is based on several lines of experimental evidence. First, the rate constants for intramolecular ET estimated by simulation of the 1D IR line shapes in the ν(CO) region, extend up to ca. 3×10^{12} s^{-1} in solvents such as acetonitrile. This is approaching the average pre-exponential frequency factors in normal Arrhenius-type rate expressions, suggesting that the activation barriers for these reactions are approaching zero,[13,20] the class III limit. Second, k_{ET}, estimated by simulation of the 1D IR lineshapes in seven polar solvents, showed a strong correlation with solvent dynamics,[21] especially Maroncelli's t_{1e},[22] which is considered the fast component of the total solvent dynamic response to changes in the electronic environment. This suggested that the 1D IR line shapes were being controlled by

Received: March 12, 2011
Published: May 11, 2011

dx.doi.org/10.1021/ja2022784 | J. Am. Chem. Soc. 2011, 133, 8721–8731

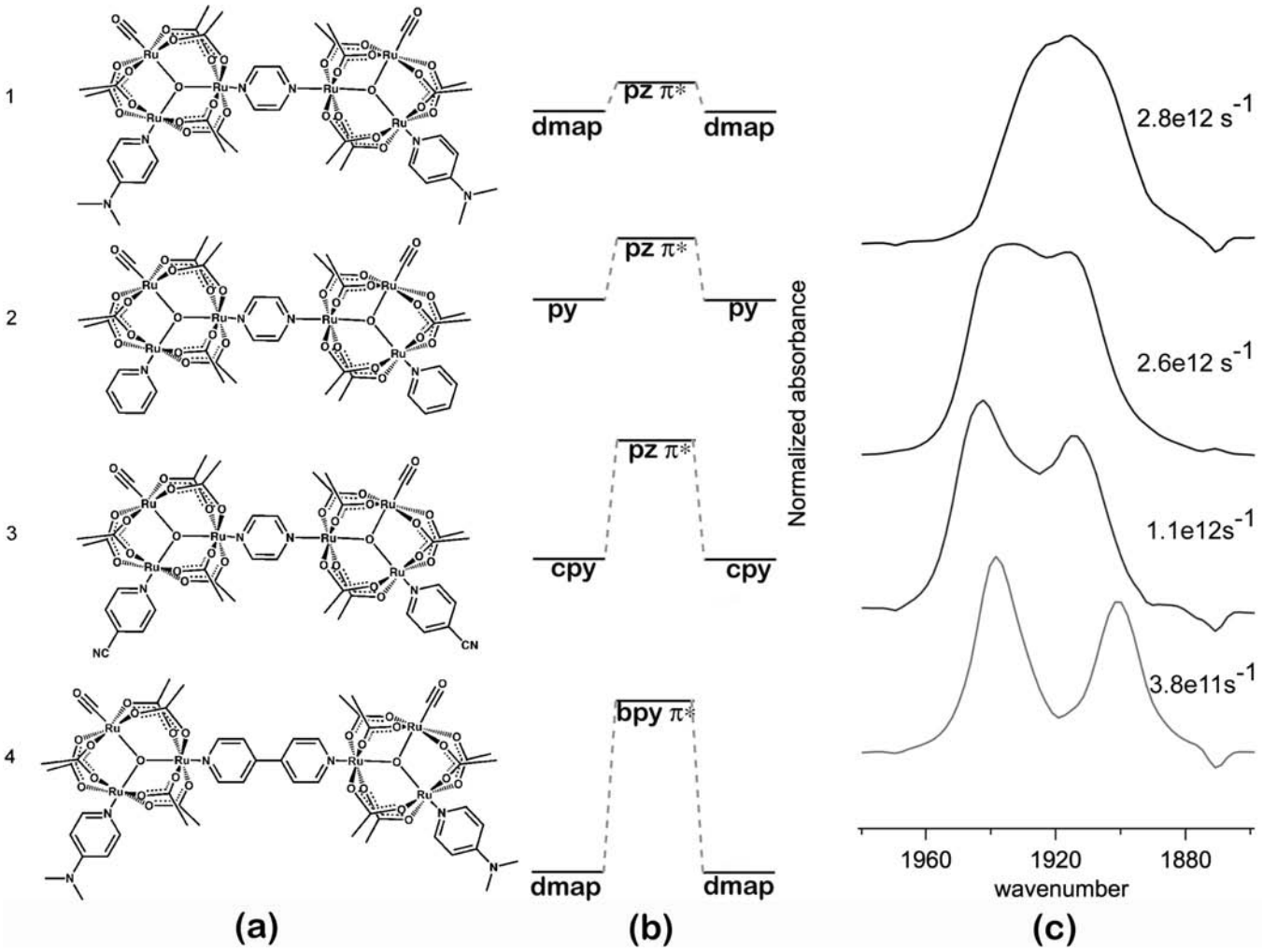

Figure 1. (a) The complexes of the type $[Ru_3(\mu_3\text{-}O)(OAc)_6(CO)(py)-(\mu_2\text{-}BL)-Ru_3(\mu_3\text{-}O)(OAc)_6(CO)(py)]^{-1}$, where BL = 1,4-pyrazine and py = 4-dimethylaminopyridine (**1**), pyridine (**2**), or 4-cyanopyridine (**3**) and BP = 4,4′-bipyridine and py = 4-dimethylaminopyridine (**4**); (b) qualitative molecular orbital representations of relative energies of Ru_3 d-orbitals (LUMO for neutral species) and bridging ligand π^* orbitals; (c) ν(CO) region of the IR spectra of the mixed valence ions $\mathbf{1}^-$—$\mathbf{4}^-$ in acetonitrile at 298 K, and rate constants, k_{ET}, estimated by simulation of the IR line shape.

dynamics on the picosecond time scale, as expected for nearly barrierless ET. Third, freezing the solvents led to complete coalescence of the ν(CO) line shapes, and the rate constants that clearly were different in fluid solution became the same at the solvent freezing points and did not change upon further cooling. The observed *acceleration* of k_{ET} at the solvent freezing points[16] was explained by a localized-to-delocalized transition where the external solvent dynamical motions become weighted less than (faster) internal modes of vibration.[23] On the basis of these studies, we have proposed a revised definition of borderline class II/III mixed valence complexes as those in which the solvent dynamical parameters control rates of ET and tend to localize otherwise delocalized electronic states.[24]

Here, we describe the intervalence charge transfer (IVCT) spectra of these borderline class II/III mixed valence complexes. We show that the spectra are best described by a three-state semiclassical model[13] that includes both Ru_3 redox center states and a state for the bridging ligand. Only such a three-state model captures the fact that the mixed valence ions $\mathbf{1}^-$—$\mathbf{4}^-$ display *two* IVCT transitions in the near-infrared (NIR) electronic spectra. Further, we show how such three-state mixed valence complexes present temperature and solvent dependences that provide significant information about the degree of electronic delocalization. We are not aware of other systems that offer the opportunity to study optically induced ET in electronic ground states that are delocalized up to the limit that solvent dynamics will allow. The detailed study of three-state mixed valency in these systems offers the opportunity to refine our understanding of the general question of electronic delocalization.

EXPERIMENTAL SECTION

Synthesis of all compounds has been reported previously in the literature.[18] Acetonitrile and methylene chloride solvents used in this study were obtained from a custom dry solvent system. All other solvents were distilled over sodium benzophenone and degassed before use. Cobaltocene and decamethylcobaltocene were used as received from Strem and Sigma Aldrich, respectively. Chemical reductions were performed under an inert atmosphere. For complexes $\mathbf{1}^-$ and $\mathbf{4}^-$, decamethylcobaltocene was added stoichiometrically. For complexes $\mathbf{2}^-$ and $\mathbf{3}^-$, cobaltocene was added stoichiometrically to produce the monoanion.

All UV—vis—NIR spectra were collected with a Shimadzu UV 3600. Samples were contained in Specac sealed liquid IR cells with CaF_2

dx.doi.org/10.1021/ja2022784 |*J. Am. Chem. Soc.* 2011, 133, 8721–8731

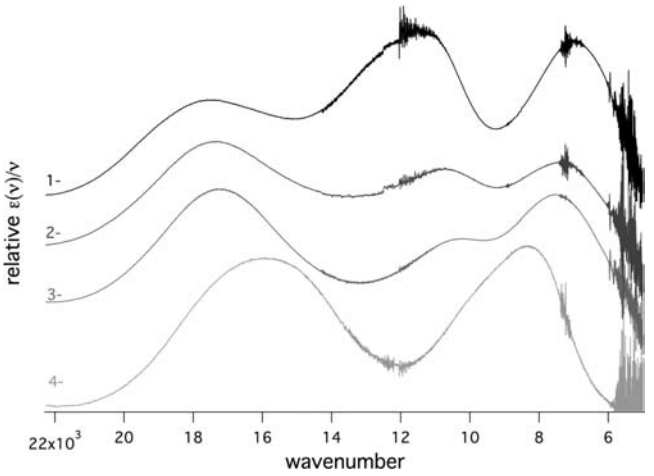

Figure 2. Near-infrared (NIR) spectra of $1^{-}-4^{-}$ in acetonitrile at 298 K. IVCT band energies are given in Table 1.

Table 1. MBCT and MMCT Band Energies[a] of $1^{-}-4^{-}$ in Acetonitrile and Methylene Chloride at 25° C[b]

	acetonitrile		methylene chloride	
complex	MBCT	MMCT	MBCT	MMCT
1^{-}	11100	6950	11130	6645
2^{-}	10560	7050	10350	6820
3^{-}	10090	7300	10050	7310
4^{-}	9530	7920		

[a] Energies in units of wavenumbers. [b] Extinction coefficients and integrated band intensities can be found in the Supporting Information.

windows and path length of 1.00 mm. Temperature-dependent studies were carried out in a Specac cryostat cell. Spectral deconvolution of NIR spectra was carried out in IGORpro.

All DFT calculations of were performed in Jaguar version 3.5 (1998 Schrodinger, Inc.)[25] running on a single Pentium III processor. Calculations of monomeric ruthenium clusters were performed with B3LYP/LACVP**[26] level of theory and those of the bridging ligand pyrazine with B3LYP/6-31G*. Further details concerning calculations can be found in the Supporting Information.

RESULTS AND DISCUSSION

The Near-Infrared (NIR) Electronic Absorption Bands. Figure 2 shows the NIR region of the electronic spectra of $1^{-}-4^{-}$ in acetonitrile at 25 °C. The highest energy band that appears at 16 000 (4^{-}) to 18 000 cm^{-1} (1^{-}) is an intracluster metal-to-ligand-charge-transfer (MLCT) transition. A similar band is observed in the isolated $[Ru_3(\mu_3\text{-}O)(OAc)_6(CO)(py)_2]$ trimers, and neutral dimers-of-trimers.[17] The observed trend in the increasing energy of this band in the series $3^{-} < 2^{-} < 1^{-}$ tracks the increasing π^* energies of the ancillary pyridine ligands dmap > py > cpy. The MLCT bands at 16 000−18 000 cm^{-1} will not be considered further here. It is the two other bands that appear in the NIR spectra that are of interest. These two bands appear well-separated at 11 000 and 7000 cm^{-1} in the spectrum of 1^{-} and extensively overlapped in the spectrum of 4^{-}. Each spectrum was simulated by fitting Gaussian band shapes in order to extract energies for electronic transitions. In the case of 4^{-}, the two overlapping bands were fit to two Gaussians, however, due to increasingly pronounced low-energy cutoff in more highly coupled species $1^{-}-3^{-}$ fitting to a single Gaussian was not possible. The best fitting method was to place a small Gaussian centered at the absorbance maximum of the asymmetric peak. This has the net effect of introducing asymmetry to the band shape. Energies of high-energy and low-energy bands in acetonitrile at 298 K for $1^{-}-4^{-}$ are given in Table 2.

Table 2. Energies[a] of MBCT and MMCT Bands of Mixed Valence Complex 3^{-} in Four Different Solvents[b]

solvent	MBCT	MMCT
acetonitrile	10090	7300
methylene chloride	10050	7310
dimethyl sulfoxide	10100	7310
butyronitrile	10450	6960

[a] In wavenumbers. [b] The difference in energies between acetonitrile an butyronitrile is small, 3.5% (MBCT) and 4.7% (MMCT).

The IVCT spectra of $1^{-}-3^{-}$ have been assigned with varying degrees of success since their original report in 1997.[18] In the first discussion of the appearance of two IVCT bands, the higher energy band was assigned as the intercluster IVCT band, but within the context of a two-state Marcus−Hush model, and the lower energy band was assigned as intracluster IVCT.[19] In 2006, we proposed three-state (two Ru_3 sites + bridge) and five-state (two Ru_3 sites + bridge + two ancillary pyridine) models based on the vibronic coupling model originally developed by Ondrechen[9,27,28] to describe the IVCT spectra of $1^{-}-3^{-}$[29] and ten related complexes.[17] The three- and five-state vibronic coupling models captured the appearance and trends of the two IVCT bands of complexes $1^{-}-4^{-}$ and many more, but they did not provide a theoretical framework to describe the localized-to-delocalized transition or to begin to understand the effects of solvent and temperature. Here, we apply a semiclassical three-state model developed by Brunschwig, Creutz, and Sutin[13] that is parametrized in terms of donor−acceptor coupling, H_{AB}, donor−bridge coupling, H_{AC}, and the vertical energy separation between the donor and the bridge state, ΔG_{AC}. We will show how this model behaves through a nearly complete localized-to-delocalized transition and how it can be combined with solvent models to describe temperature and solvent effects on IVCT spectra at the class II/III borderline.

Three-State Model of Mixed Valency. Semiclassical Marcus−Hush theory has been used with much success in the description of mixed valence systems.[6,20,30,31] The three-state model, developed by Brunschwig, Creutz, and Sutin, closely follows the two-state Marcus−Hush model but employs a third state to represent the bridging ligand.[13] Though we will focus on the electron transfer aspects of this model, hole transfers are also ubiquitous in mixed valency, for example, in donor−bridge−acceptor systems,[32] DNA,[33,34] polymers,[35] and quantum dots.[36,37] There are, to our knowledge, a very limited number of studies that follow a multistate hole transfer analysis, and there may be many exciting opportunities in that direction.

Figure 3a,b shows potential energy surfaces for two- and three-state models, respectively, along the asymmetric reaction coordinate. Potential energy surfaces (PESs) map the energies along the nuclear coordinate, composed of internal nuclear coordinates and outer sphere solvent coordinates that contribute to the mixed valence character. When the bridge state lies higher in energy than the donor and acceptor states, the three-state

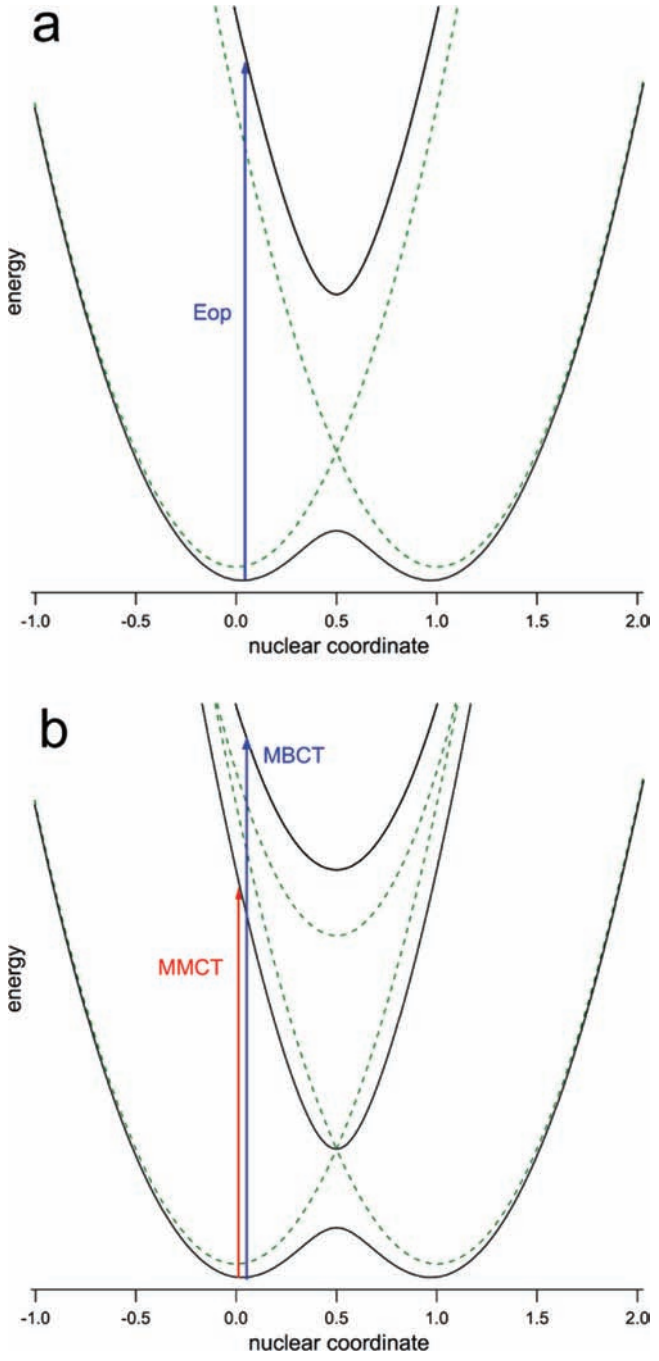

Figure 3. (a) Diabatic (green dash) and adiabatic (black line) potential energy surfaces of a two-state mixed valence system. E_{op} is the optical excitation energy from donor to acceptor surfaces. (b) Diabatic and adiabatic potential energy surfaces for a three-state system, where a surface is included for the bridging ligand state. MMCT corresponds to the energy of the optical transition between donor and acceptor, while MBCT corresponds to the energy of the optical transition from donor to bridge.

model predicts PESs such as those in Figure 3b. In the three-state system, there are three electronic coupling constants, H_{ab}, H_{ac}, and H_{bc}; however in a symmetric system $H_{ac} = H_{bc}$ and only two electronic coupling parameters need to be considered; donor−acceptor coupling is defined as H_{ab}, and donor−bridge coupling as H_{ac}. Electronic coupling between the donor−bridge−acceptor assembly brings about three adiabatic states of consequence: ground and excited state states involving the two metal (Ru_3) units (having mainly metal cluster character), and an excited state in which bridge character predominates. It is noteworthy that increasing either donor−acceptor coupling, H_{ab}, or donor-bridge coupling, H_{ac}, increases the adiabaticity of the three PESs: as the energy of the ground-state PES is stabilized, the activation energy at the classical turning point is decreased, and the minima on each side move closer together. Additionally, as H_{ac} increases the excited-state bridge PES is shifted to higher energy. Despite the similarities between the two models, the trends predicted for IVCT bands are quite different.[4,13,20] Most notably, the three-state model predicts two IVCT transitions. When the bridging ligand state is higher in energy than the two metal-based states, the low-energy transition is metal-to-metal-charge-transfer (MMCT) in character, and the high-energy transition is metal-bridging ligand-charge-transfer (MBCT), Figure 3b. It is how these two IVCT transitions respond to increasing electronic coupling that contrasts most strongly with conventional two-state behavior.

Figure 4 shows a series of three-state PESs with increasing electronic communication. It is expected that as electronic coupling between cluster and bridge states increases, the MBCT band will *increase* in energy, and the MMCT band will *decrease* in energy until delocalization is achieved.[13] In the case of the MBCT band, the trend is the same as an IVCT band of a two-state system, but the trend of the MMCT band is the opposite. This trend in energies of MMCT and MBCT bands will continue until the system is fully delocalized (class III), at which point the MBCT band is predicted to vanish and the MMCT band is predicted to become increasingly narrow and intense.[13] Further predictions for three-state mixed valency include intensification, narrowing, and increased band asymmetry on the low-energy side of IVCT band shapes as complexes become increasingly delocalized.[13] The notion that the MBCT band vanishes once delocalization has been achieved was challenged by a recent study of highly electronically coupled class III systems.[38] In this study, Lear and Chisholm investigated the intervalence properties of a series of delocalized mixed valence complexes and found that not only were MBCT bands present, but they exhibited quite large intensities. Their findings contradict the three-state model where the MBCT intensity is predicted to vanish at the point of delocalization. The prediction of a vanishing MBCT band is a valid outcome of the three-state model when only electronic coupling between donor and bridge (redox metal state to bridging ligand state) is considered, which implies that MBCT bands have no MMCT character and *vice versa*. However, in real systems, especially those that possess large degrees of electronic coupling, there is likely mixing of donor, bridge, and acceptor states, and the MBCT band will thus possess at least some MMCT character. In this case, the MBCT band is *not* expected to vanish at the point of delocalization.

To date, it has proven very difficult to classify borderline mixed valence complexes by IVCT band shape character alone, and further spectroscopic investigation is usually required. The mixed valence complexes $\mathbf{1}^-$−$\mathbf{3}^-$ do exhibit borderline behavior in the IR spectra,[16,39] but coalescence of IR spectra only indicates that electronic delocalization has been achieved on a picosecond vibrational time scale, which is not necessarily an indication of collapse of the ground-state PES to a single minimum. We consider next how the three-state model for mixed valency describes the transition toward delocalization and the solvent and temperature dependence along the way.

dx.doi.org/10.1021/ja2022784 |*J. Am. Chem. Soc.* 2011, 133, 8721–8731

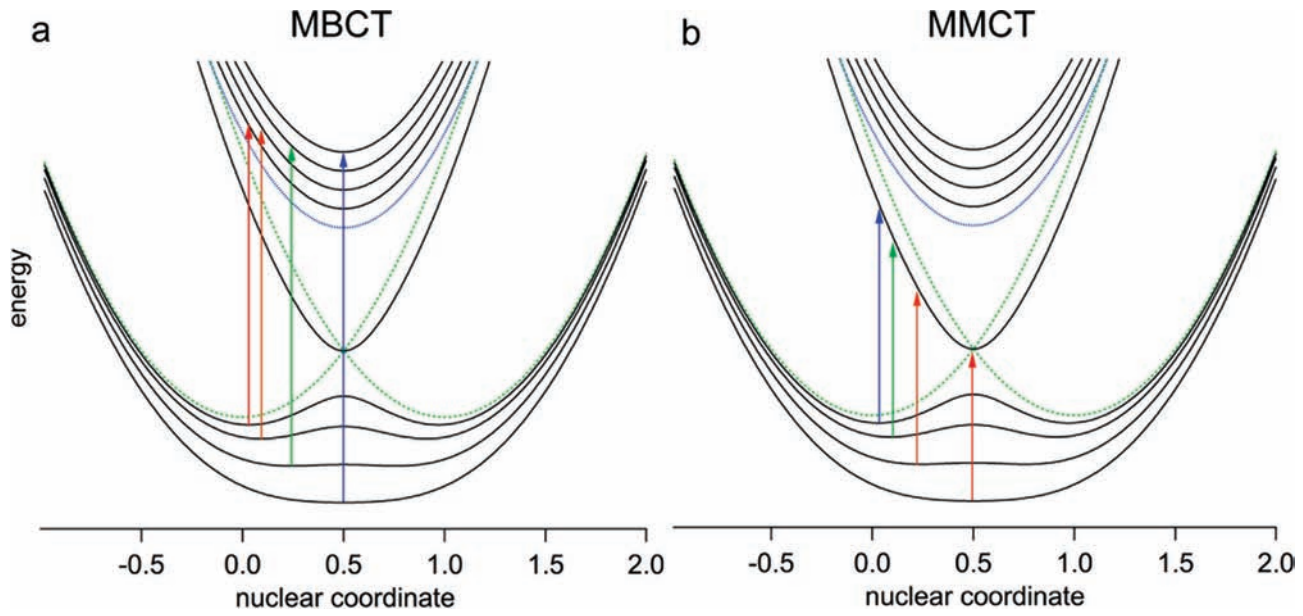

Figure 4. (a) A series of potential energy surfaces showing the effect of increased coupling on the vertical energy difference or metal-to-bridge-charge-transfer (MBCT) energy of adiabatic ground state and bridge state. Increased coupling leads to more energetic MBCT bands. (b) A series of potential energy surfaces showing the effect of increased coupling on the vertical energy difference or metal-to-metal-charge-transfer (MMCT) energy of adiabatic ground state and excited metal state. Increased coupling leads to less energetic MMCT bands.

Interpretation of NIR Spectra within the Three-State Model. The energies of the IVCT bands of complexes $\mathbf{1}^-$–$\mathbf{4}^-$ are tabulated in Table 1. Previous studies of these complexes have led to the conclusion that the bridging ligand π^* levels lie higher in energy than the d-orbitals involved in the mixed valence states, as shown in Figure 1b.[17,19] Thus, the three-state PESs of Figures 3 and 4 are appropriate in the description of $\mathbf{1}^-$–$\mathbf{4}^-$. Previous studies also indicate the order of increasing electronic communication in the mixed valence ions as $\mathbf{4}^- < \mathbf{3}^- < \mathbf{2}^- < \mathbf{1}^-$. This is based on the larger splittings $\Delta E_{1/2}$ of the reversible reduction processes between the (0/−1) and (−1/−2) states that correspond formally to $Ru_3^{III,III,II}$–BL–$Ru_3^{III,III,II}$/$Ru_3^{III,II,II}$–BL–$Ru^{III,III,II}$ (0/−1) and $Ru_3^{III,II,II}$–BL–$Ru_3^{III,III,II}$/$Ru_3^{III,II,II}$–BL–$Ru_3^{III,II,II}$ (−1/−2), where the −1 state is the intercluster mixed valence state of interest. The increasing order of electronic communication is also apparent in the IR spectra in the ν(CO) region, which shows increasing spectral coalescence in the order $\mathbf{4}^- < \mathbf{3}^- < \mathbf{2}^- < \mathbf{1}^-$, corresponding to increasing degrees of electronic delocalization on the vibrational time scale. If the two bands between 6000 and 12 000 cm^{-1} (Figure 2) are considered to be three-state IVCT bands, their behavior with increased electronic communication can be explained well. From $\mathbf{1}^-$ to $\mathbf{3}^-$, there is a gradual decrease in electronic communication, and the high-energy IVCT band moves to lower energy as the low-energy IVCT band moves to higher energy. That is to say, the high-energy IVCT band behaves like a three-state MBCT band, and the low-energy IVCT band behaves like a MMCT band. The mixed valence ion $\mathbf{4}^-$ has a 4,4′-bipyridine in place of pyrazine as the bridging ligand, and this leads to a sharp decrease in electronic communication, as gauged by electrochemical and IR spectroscopic data.[19] Extensive overlap of the MBCT and MMCT bands is observed for this dimer. The energetic separation between MMCT and MBCT bands is expected to be the smallest with less strongly electronically coupled systems. The assignment of the NIR spectra of $\mathbf{1}^-$–$\mathbf{4}^-$ in the 6000–12 000 cm^{-1} region as MBCT (high-energy IVCT band) and MMCT (low-energy IVCT band) is also consistent with previous resonance Raman studies.[40,41] Resonance Raman spectra of $\mathbf{1}^-$–$\mathbf{3}^-$ showed only enhancement of symmetric modes of the bridging pyrazine ligand upon excitation of the high-energy IVCT band.[40,41] It was not experimentally possible to obtain resonance Raman spectra within the low-energy IVCT band. The strong apparent vibronic involvement of the bridging pyrazine ligand modes in the high-energy IVCT band is consistent with a MBCT electronic transition, and we can be quite confident in this assignment. The lower energy IVCT bands appearing at ca. 7000 cm^{-1} are then assigned as the MMCT bands.

The three-state description of mixed valency effectively describes the trend in diverging energies of MMCT and MBCT bands in mixed valence complexes $\mathbf{1}^-$–$\mathbf{4}^-$. Recall that at the class II/III to class III (localized-to-delocalized) transition the MBCT band is expected to vanish, but we see that even in the most electronically coupled dimer, $\mathbf{1}^-$, strong MBCT intensity persists. Because of the extensive electronic communication in dimers of this study, we believe that coupling between all states can exist and MBCT band intensity will remain through a localized-to-delocalized transition. Analysis of the ν(CO) region of the IR spectra of $\mathbf{1}^-$–$\mathbf{3}^-$ led to a similar conclusion.[19] In Figure 1c, it can be seen that the ν(CO) spectra of $\mathbf{3}^-$ and $\mathbf{2}^-$ are not coalesced, and that for $\mathbf{1}^-$ is nearly but not fully coalesced. This has been interpreted in terms of extensive but incomplete delocalization.[19] Next, we consider how the MBCT and MMCT bands of the three-state model respond to solvent properties and temperature.

Solvent Dependence of Three-State MBCT and MMCT Bands. Most commonly, a distinction is made between class II and class III by a mixed valence complex's solvatochromic behavior of the IVCT bands.[6,15] This stems from the fact that the energy required for solvent reorientation will contribute to the total reorganization energy. Reorganization energy in mixed valence systems is composed of a sum of inner sphere and outer sphere components and is commonly represented by $\lambda_{tot} = \lambda_i + \lambda_o$. The inner sphere component, λ_i, accounts for the energy required for collective nuclear displacements and bond vibrations

dx.doi.org/10.1021/ja2022784 |J. Am. Chem. Soc. 2011, 133, 8721–8731

that are coupled to charge transfer. The outer sphere component, λ_o, accounts for energy required to reorient the solvent following redistribution of charge on the mixed valence species. Descriptions of how the solvent environments interact with the exchanging electron in class II, class II/III "borderline", and class III mixed valence systems follow.[6] For a class II species, the exchanging electron and solvent are localized. In a class III mixed valence complex, the electron is delocalized and solvent is averaged. At the class II/III localized-to-delocalized transition, the electron is localized and solvent is averaged. But, solvent motions that are averaged with respect to a localized electron imply that solvent motion is either faster than electron exchange or uncoupled to it. For complexes $\mathbf{1}^-$—$\mathbf{3}^-$, we have shown that this cannot be the case. Solvent and temperature dependence studies of $\mathbf{1}^-$—$\mathbf{3}^-$ have shown that the rates of ET are strongly correlated to solvent dipolar reorientation times.[16,21,39] A particularly relevant question then is: how do three-state mixed valence MBCT and MMCT bands respond to solvent through the class II/III transition? Table 1 summarizes the MBCT and MMCT band energies of $\mathbf{1}^-$—$\mathbf{4}^-$ in acetonitrile and methylene chloride at 25 °C.

The data show that there is only a small variation in band energies of the four mixed valence ions in methylene chloride and acetonitrile. In the case of complexes $\mathbf{1}^-$—$\mathbf{3}^-$, it can be seen that band energies of MBCT and MMCT are in general slightly greater in acetonitrile than in methylene chloride. This is consistent with acetonitrile having a larger solvent reorganization energy than methylene chloride; however, the differences are so small that they would not be expected to significantly change the shape of a potential energy surface. Complex $\mathbf{3}^-$ was further studied in dimethyl sulfoxide and *n*-butyronitrile, and again only a small variation in energies was observed (Table 2). The weak solvent dependence of the IVCT bands of $\mathbf{1}^-$—$\mathbf{3}^-$ are consistent with very low barriers for ET and extensive delocalization. A note of caution should accompany this analysis. When these complexes are assessed by traditional Marcus—Hush analysis of their band shape energies, the degree of delocalization and rates of electron transfer are greatly underestimated.[42] The weak solvent dependence of the IVCT bands of $\mathbf{1}^-$—$\mathbf{3}^-$ is consistent with complexes that are highly electronically coupled. A source of considerable confusion is that the use of a traditional two-state Marcus—Hush treatment leads to a class II assignment, based on the energy of the IVCT bands of $\mathbf{1}^-$—$\mathbf{3}^-$, but assignment as class III based on their nearly solvent-independent response. It is preferable to establish a more quantitative classification of class II/III, rather than simply noting that these complexes show some delocalized and some localized behavior. We know from IR vibrational spectroscopy that rates of electron transfer are on the picosecond time scale, which points to nearly barrierless electron transfer and rate constants that are controlled by the pre-exponential frequency factor in the rate expression.[16,39] This underscores the importance of understanding the dynamic contributions of solvent to mixed valence character in highly coupled complexes at the borderline of delocalization.

Temperature Dependence of Three-State MBCT and MMCT Bands. We turn now to the temperature dependence of the MBCT and MMCT bands. A previous study from our laboratory showed non-Arrhenius temperature dependence of rates of electron transfer for $\mathbf{1}^-$—$\mathbf{3}^-$ in acetonitrile and methylene chloride, that is, the rates of ground-state intramolecular electron transfer were observed to increase as the temperature of solutions was decreased.[16,39] We described this as a localized-to-delocalized transition as solvent modes were decoupled from the electron transfer reaction. The question of how the MBCT and MMCT bands respond to temperature is now addressed. It will be important in the following analysis to consider parameters used to describe the energetic landscape for the mixed valence system and how they can be affected, if at all, by temperature. Parameters that are fundamental to the energetic description are the electronic coupling parameters, H_{ab} and H_{ac}, ΔG_{ac}, and the reorganization energy, λ. Of these, H_{ab}, H_{ac}, and ΔG_{ac} are not expected to change with temperature, because they are intrinsic electronic parameters of the mixed valence complex.[43] The reorganization energy, specifically the solvent reorganization energy, is expected to change with temperature. The high-frequency vibrational modes of the complex, which contribute to the inner sphere reorganization energy, λ_i, are not expected to change significantly in the temperature range of this study, which leaves the outer sphere reorganization energy, λ_o, as the sole temperature-dependent parameter of interest.

The solvent reorganization energy describes the energy required for solvent dipoles to reorient in order to accommodate change in dipole moment of the mixed valence complex following an electron transfer event. The ubiquitous continuum treatment of solvent from semiclassical Marcus—Hush theory has been used with success for the description of many mixed valence systems.[44] Recent work by Matyushov and others has described some shortcomings of the continuum theory in describing solvent reorganization energy.[45] A study by Zimmt, Waldeck, and coworkers addresses the differences between Marcus continuum and Matyushov molecular solvation theories and their effectiveness in describing solvent reorganization energy.[43] Their findings are pertinent to the discussion at hand because they describe the different outcomes of temperature dependence of λ_o when considering solvation from a continuum or molecular perspective. The conventional Marcus—Hush continuum model assumes a dipolar continuum surrounding a "hard sphere" donor—acceptor assembly. The expression for reorganization energy takes into account that optical (ε_{op}) and static (ε_s) dielectric constants are temperature-dependent. The solvent-dependent portion, or the Pekar factor,[46] describes the solvent dipolar reorientation near the donor—acceptor interface. This model predicts that for strongly polar solvents, like acetonitrile, as temperature decreases the solvent reorganization energy decreases. Matyushov's molecular solvation theory extends the continuum model to include the longitudinal response of the solvent in addition to the reorientational component. Both rotational and longitudinal aspects are temperature-dependent, but calculations reveal that their contributions are not equal in magnitude.[43,45] The rotational component has a temperature dependence determined (as in continuum theory) by the Pekar factor, and the longitudinal component depends on the thermal expansivity of the solvent. The net result is that Matyushov's solvation theory predicts an increase in solvent reorganization energy with decreasing temperature in strongly polar solvents, which is in disagreement with predictions of continuum theory. When longitudinal and rotational components are considered separately, however, the molecular solvation model predicts that the rotational component decreases with temperature. The longitudinal component is expected to increase with decreasing temperature and with greater magnitude than the rotational component. When the two contributions are considered together, an overall *increase* in solvent reorganization energy as temperature decreases is predicted.

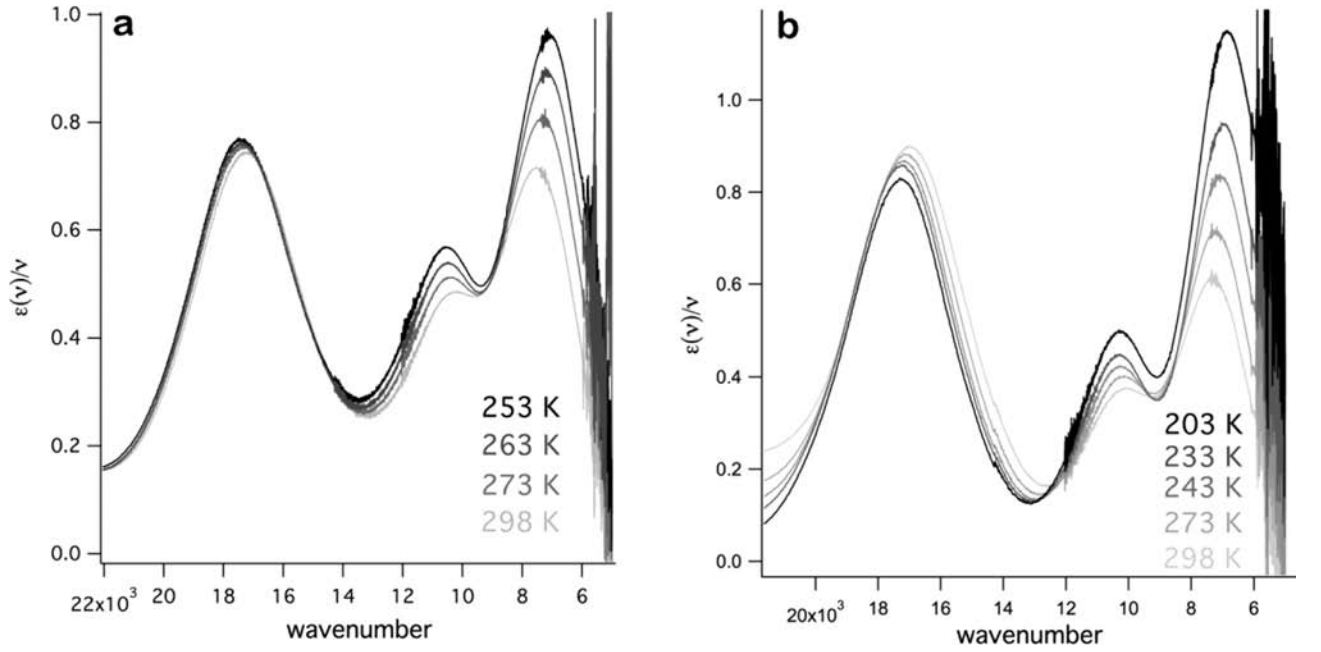

Figure 5. Spectra of $\mathbf{3}^-$ collected in acetonitrile (a) and methylene chloride (b). An increase in MBCT and decrease in MMCT band energies is observed in both solvents.

Changes in IVCT bands of $\mathbf{1}^-$—$\mathbf{4}^-$ in acetonitrile and methylene chloride were followed as a function of temperature. Figure 5 shows the spectra of $\mathbf{3}^-$ in acetonitrile and methylene chloride at increasingly colder temperatures. What can be seen is that as the temperature of the solution is decreased, the bands intensify and change in energy. Specifically, the MMCT transition decreases in energy and the MBCT transition increases in energy. The divergence in energies of the two transitions is reminiscent of the behavior exhibited by $\mathbf{1}^-$—$\mathbf{4}^-$ as electronic communication increases (*vide supra*). This trend is consistent with increasingly delocalized behavior as the temperature is decreased. Additionally, the MMCT bands increase in intensity by 50% in acetonitrile and 130% in methylene chloride, Figure 5. An increase in intensity of the MMCT band is predicted by the three-state model for a system that is approaching delocalization.[13] This observation of increasingly delocalized behavior as the temperature decreases is in accord with our observations of temperature dependence on ground-state electron transfer in IR studies of the ν(CO) spectra.[16,39]

Changing the reorganization energy in a mixed valence system, inner or outer sphere, will alter the landscape of potential energy surfaces describing a mixed valence species. Increasing the reorganization energy and treating H_{ab}, H_{ac}, and ΔG_{ac} as constants will cause the activation barrier along the symmetric coordinate to increase in a PES, and a mixed valence species will take on more localized character. Conversely, decreasing the reorganization energy will allow a mixed valence species to take on more delocalized character. Figure 6 shows three sets of potential energy surfaces generated for a two-state system where only the reorganization parameter has been changed. All other factors being equal, when the reorganization energy is smaller, the potential energy surface is more adiabatic. The resultant spectra of $\mathbf{3}^-$ are consistent with a small decrease in reorganization energy as the temperature is decreased.

From the standpoint of the classic Marcus continuum theory, this result is in agreement; however from the more descriptive Matyushov solvation theory, there is clearly a discrepancy.

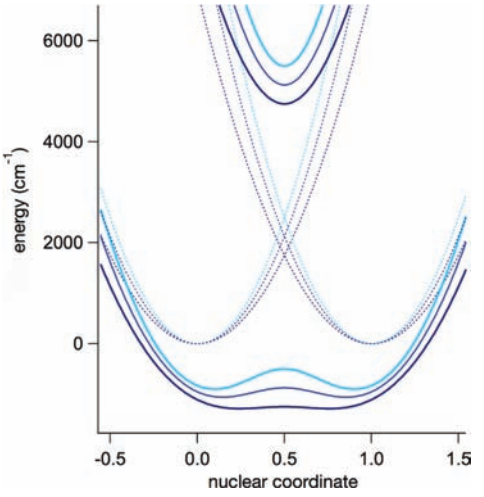

Figure 6. Three sets of potential energy surfaces where the electronic coupling constant is held at 3000 cm^{-1} and the reorganization energy is varied. λ is (dark blue) 7000 cm^{-1}, (medium blue) 8500 cm^{-1}, and (cyan) 10000 cm^{-1}.

Molecular solvation theory predicts a net increase in solvent reorganization energy as the temperature is decreased. A key point, however, is that molecular solvation theory predicts that the rotational component to the net solvent reorganization energy will *decrease* as temperature decreases. Comparison of ET lifetimes versus solvent dynamic parameters elucidated that the rotational solvent response is a large contribution to the mixed valence character of complexes on the borderline of delocalization. Specifically, we have shown that rates of electron transfer in complexes $\mathbf{1}^-$—$\mathbf{3}^-$ depend strongly on solvent dipolar reorientation, [16] and therefore it stands to reason that the energy associated with these motions will greatly contribute to the outer sphere reorganization energy of these complexes. Likewise, rates

dx.doi.org/10.1021/ja2022784 |*J. Am. Chem. Soc.* 2011, 133, 8721–8731

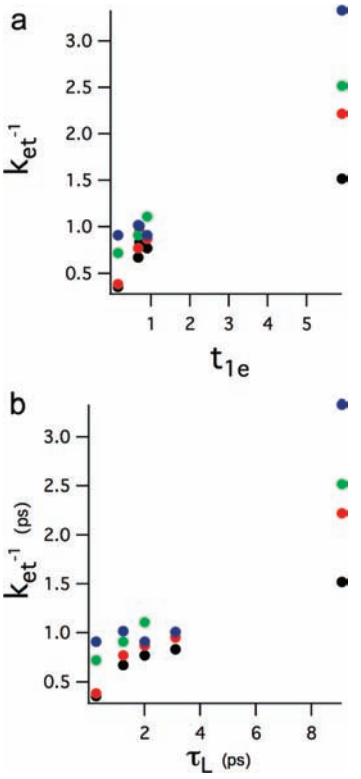

Figure 7. (a) Solvent dipolar reorientation time versus complex electron transfer lifetime for $\mathbf{1}^-$ (black dots), $\mathbf{2}^-$ (red dots), $\mathbf{3}^-$ (blue dots), and $[Ru_3(\mu_3\text{-O})(OAc)_6(CO)(py)-(\mu_2\text{-pyrazine})-Ru_3(\mu_3\text{-O})(OAc)_6(CO)(py)]^{-1}$ (green dots) where py = 2-cyanopyridine (average R^2 = 0.860). The values for solvent (t_{1e}) are as follows: acetonitrile (0.15 ps), dimethylformamide (0.67 ps), tetrahydrofuran (0.7 ps), dimethylsulfoxide (0.9 ps), and hexamethylphosphoramide (5.9 ps).[22] (b) Plotted are solvent longitudinal response times,[47,48] τ_L, versus electron transfer lifetime for the same four dimers (average R^2 = 0.605). The values for solvent (τ_L) are as follows: acetonitrile (0.25 ps), dimethylformamide (1.23 ps), tetrahydrofuran (3.1 ps), dimethylsulfoxide (2 ps), and hexamethylphosphoramide (9.09 ps).

of electron transfer in $\mathbf{1}^-$–$\mathbf{3}^-$ do not correlate strongly to slow (longitudinal) solvent response and as such the longitudinal component to the net solvent reorganization energy, so it is expected that this aspect of the outer sphere reorganization energy will not be as important in $\mathbf{1}^-$– $\mathbf{3}^-$. Figure 7 compares the solvent longitudinal response and the solvent dipolar reorientation time versus electron transfer lifetimes for four symmetric dimers.

The correlation is poorer for the longitudinal solvent response vs electron transfer lifetime than it is for the solvent dipolar response (t_{1e}) vs the electron transfer lifetime. This is evidence that electron transfer in these deeply adiabatic systems is strongly influenced by solvent dipolar reorientation but less so by solvent longitudinal response. This makes sense when considering the time scales of the different solvent motions and rates of ET. Longitudinal motions have a longer time scale than the ET event in $\mathbf{1}^-$–$\mathbf{3}^-$. From a dynamic perspective, ET has already proceeded before solvent longitudinal motion can respond. In contrast, solvent dipolar reorientation times are on the same time scale as ET in these systems, and ET does not proceed until all the nuclear coordinates and solvent dipoles are aligned favorably. By this rationale, it appears that the dipolar reorientation portion of the molecular solvation theory is the component

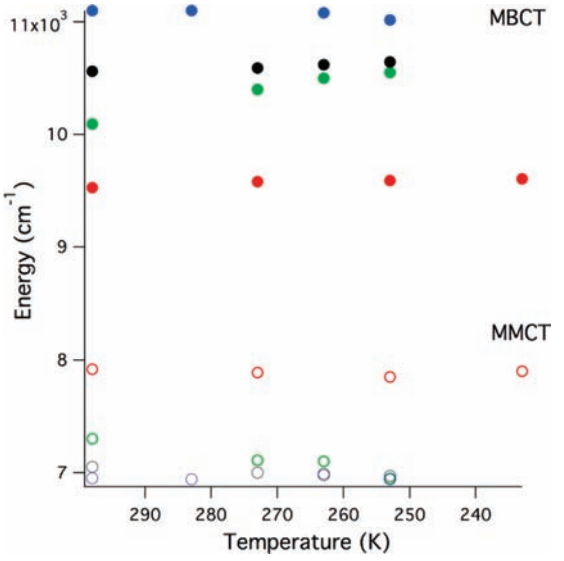

Figure 8. Energies of MMCT (filled circles) and MBCT (open circles) bands as temperatures are decreased for the four dimers in this study: $\mathbf{1}^-$ (black), $\mathbf{2}^-$ (blue), $\mathbf{3}^-$ (green), and $\mathbf{4}^-$ (red).

of greater importance when the system is nearly delocalized. With this effect included, current theories of solvation will properly account for more delocalized behavior on lowering the temperature. The plot in Figure 8 summarizes band energies versus temperature for $\mathbf{1}^-$–$\mathbf{4}^-$ in acetonitrile. Complexes $\mathbf{2}^-$ and $\mathbf{1}^-$ show analogous temperature-dependent behavior in their MMCT and MBCT band energies, but $\mathbf{2}^-$ to a much lesser degree and with almost no change for $\mathbf{1}^-$. From Figure 8, it can be seen that MMCT and MBCT bands of $\mathbf{4}^-$ are independent of temperature. Compound $\mathbf{4}^-$ is the least electronically coupled dimer in this study and is a class II, electron localized system. By convention, it is expected that the IVCT band of a class II ion like $\mathbf{4}^-$ will be solvent-dependent, so it may seem unusual that there is no observed temperature dependence. Temperature-dependent IR spectra of $\mathbf{4}^-$ show no change in ν(CO) band shape and no change in rate constant for electron transfer. This is in contrast to $\mathbf{1}^-$, $\mathbf{2}^-$, and $\mathbf{3}^-$, which all exhibit rate acceleration upon freezing of the solvent. This difference in behavior of $\mathbf{4}^-$ stems from the fact that the electronic ground state is localized with or without solvent dynamics in play. The more highly coupled systems are localized when solvent dynamics are in play, and delocalized when solvent modes are uncoupled.

For systems clearly in the class II regime, solvent dynamic motions are faster than electron transfer, and they will appear averaged to the exchanging electron. Decreasing the solution temperature will change the overall outer sphere reorganization energy to a small degree; however, increased delocalization is not expected because the electron transfer is uncoupled to solvent dynamics. Since localized behavior of $\mathbf{4}^-$ persists as the solvent is frozen, temperature dependence of the IVCT spectra is not expected.

From Figure 8, it can be seen that the trend to more delocalized behavior tapers as electronic communication increases from $\mathbf{3}^-$ to $\mathbf{1}^-$. This is consistent with the series of dimers approaching the late limit of the class II/III borderline, with $\mathbf{1}^-$ being the closest to delocalized. Figure 9 shows the temperature-dependent spectra of $\mathbf{1}^-$ in acetonitrile. As the solution is cooled, the MMCT band begins to intensify and the MBCT loses intensity. This type of behavior is a predicted

dx.doi.org/10.1021/ja2022784 |*J. Am. Chem. Soc.* 2011, 133, 8721–8731

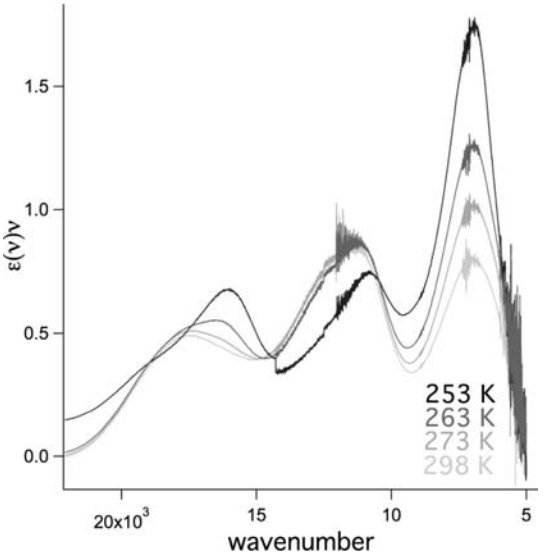

Figure 9. Compound $\mathbf{1}^-$ in acetonitrile at increasingly colder temperatures shows intensification of MMCT band and weakening of the MBCT band, consistent with a class II/III to class III transition. This dimer undergoes dramatic changes in intensity; 90% increase in MMCT and 20% decrease in MBCT intensity.

outcome of a system crossing through a localized-to-delocalized transition. We note, however, that the MBCT band is still present and bears much of its original intensity. This is *not* the predicted behavior when donor, bridge, and acceptor are treated as pure states. Due to the nature of strong electronic coupling in these systems, mixing between all states that contribute to the mixed valence character is likely and MBCT intensity should persist through the localized to delocalized transition.

Three-State Potential Energy Surfaces. A three-state model including a state for the bridge has been successfully employed to describe a number of bridged mixed valence complexes in the literature previously.[13,49,50] Potential energy surface analysis gives a snapshot of the energetic landscape of a mixed valence system, as well as the ability to simulate IVCT band shapes. The equations that generate a three-state PES along symmetric and asymmetric coordinates are given below:

$$G_a = \lambda x^2 + \lambda y^2$$

$$G_c = \lambda(x-0.5)^2 + \lambda(y-0.5)^2 + \Delta G_{ac}$$

$$G_b = \lambda(x-1)^2 + \lambda(y-1)^2$$

Here, G_a, G_c, and G_b are the energies of the donor, bridge, and acceptor states, respectively, λ is the reorganization energy, x is the symmetric nuclear coordinate and y is the asymmetric nuclear coordinate, and ΔG_{ac} is the difference in energy between the minimum of the donor (or acceptor) state and the minimum of the bridge state. In the case that electron donor, bridge, and acceptor are electronically coupled, solving the 3 × 3 secular determinant for the eigenvalues, E, will give the energies for the coupled adiabatic PES.

$$\begin{vmatrix} G_a - E & H_{ac} & H_{ab} \\ H_{ac} & G_c - E & H_{bc} \\ H_{ab} & H_{bc} & G_b - E \end{vmatrix}$$

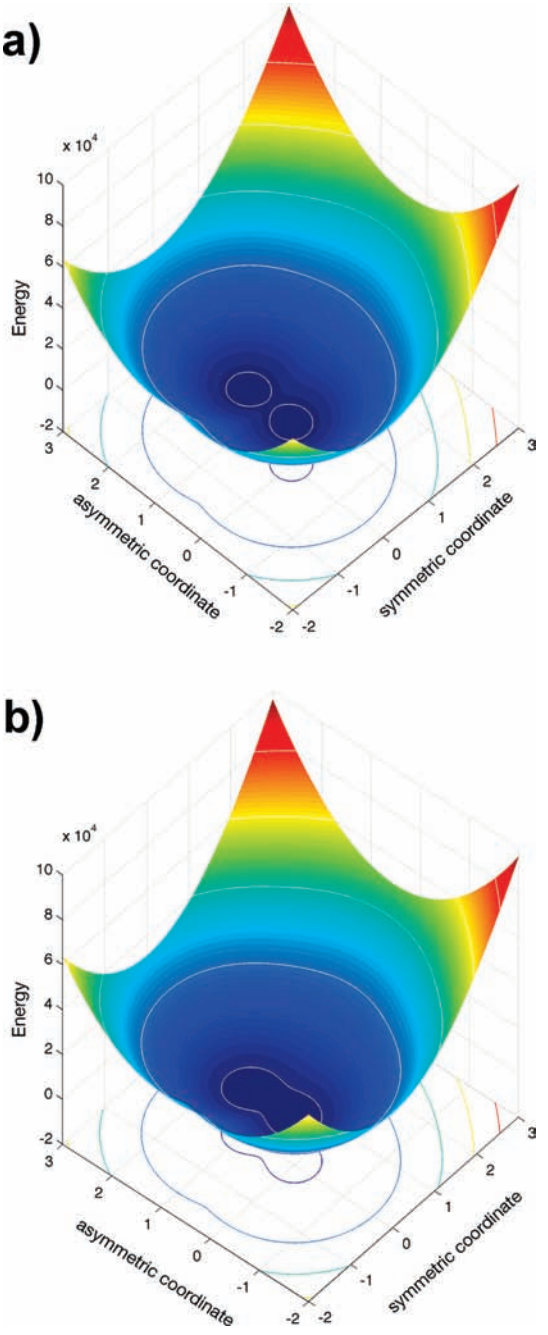

Figure 10. PES plots for **3** (a) and **1** (b). The following parameters were used to generate the ground-state surface for $\mathbf{3}^-$: λ = 8000 cm^{-1}, ΔG_{ac} = 16 700 cm^{-1}, H_{ab} = 0 cm^{-1}, H_{ac} = 4500 cm^{-1}. The following parameters were used to generate the ground-state surface for $\mathbf{1}^-$: λ = 8000 cm^{-1}, ΔG_{ac} = 14 200 cm^{-1}, H_{ab} = 0, H_{ac} = 5400 cm^{-1}. A discussion of obtaining ΔG_{ac} can be found in the Supporting Information. Estimations for electronic coupling parameters can be found in ref 33.

In order to apply a three-state treatment to our systems, values for electronic coupling constants, reorganization energy, and ΔG_{ac} will have to be determined. Electronic coupling constants have been estimated for a number of mixed valence complexes similar to $\mathbf{1}^-$—$\mathbf{3}^-$.[42] If we make the assumption that a majority of the electronic communication is between donor and bridge and that the electronic communication between donor and acceptor

dx.doi.org/10.1021/ja2022784 |J. Am. Chem. Soc. 2011, 133, 8721–8731

is negligible, the previously determined values for H_{ab} will provide a reasonable estimate for the complexes in the present study. DFT calculations were used to estimate ΔG_{ac} for $\mathbf{1}^-$ and $\mathbf{3}^-$ as 14 200 and 17 600 cm^{-1}, respectively.

PESs of the ground state along the symmetric and antisymmetric coordinate are shown for $\mathbf{1}^-$ and $\mathbf{3}^-$ in Figure 10. The ground-state surface for $\mathbf{1}^-$ is much smoother and much closer to parabolic in shape than that for $\mathbf{3}^-$, which is expected given that $\mathbf{1}^-$ has a greater degree of electronic coupling.

As can be seen, there is not a distinct minimum present for the bridging state, and the coordinate is smooth. A remarkable result of the three-state model is that even with negligible coupling between donor and acceptor, sufficient electronic coupling between donor and bridge will enable nearly barrierless ground state electron transfer. This is shown by the potential energy surfaces in Figure 10, where the activation barrier along the symmetric coordinate can be circumvented by traveling along the asymmetric coordinate.[50] This result is in accord with the ultrafast rates of electron transfer measured for these systems. Further work in this area will involve spectral simulation of NIR spectra from PES analysis.

CONCLUSIONS

The question of whether a particular system is localized or delocalized is usually best referenced to a time scale, up to class III, which represents the absolute limit of electronic delocalization. The classification of mixed valence complexes as "borderline class II/III" arose from the difficulty in locating precisely how far a particular weakly localized, adiabatic mixed valence system had to go to achieve complete class III character.[6] More recent studies of the role of solvent dynamics on delocalization have helped clarify the onset of a localized to delocalized transition.[16,24] Thus, a borderline class II/III system is one in which solvent dynamics such as solvent dipolar reorientation times tend to localize otherwise delocalized electronic states. This will generally occur when electronic coupling is large, barriers to ET are negligibly small, and the rate expression becomes dominated by internal and solvent modes that are heavily weighted in the pre-exponential frequency factor.[16] For systems that are described well by a three-state semiclassical model such as the mixed valence complexes $\mathbf{1}^-$—$\mathbf{4}^-$ in the present study, it is clear that delocalization on the time scale of the fastest (inertial) solvent motions is not sufficient to achieve complete electronic delocalization. The appearance of both the MMCT and MBCT bands in the near-IR electronic spectra is a clear indication of a transition dipole that can only be present when there is residual localization in the ground state, although whether the three-state MBCT band disappears completely at the class III limit was recently questioned.[38] In every other respect, complexes $\mathbf{1}^-$—$\mathbf{4}^-$ exhibit such a well-behaved and predictable (by the three-state model) progression through the class II/III borderline that it is tempting to use criteria from the three-state model to assign a particular system's behavior to either an "early" or "late" class II/III borderline situation. One trend that becomes immediately clear is that within the three-state description energies of MMCT and MBCT bands diverge with increased electronic communication. This relationship can be used to compare series of mixed valence complexes with varying degrees of electronic coupling, especially if the value of the electronic coupling constant is not explicitly known, as is often the case in highly electronically coupled complexes. We have also found that a study of solvent and temperature effects can reveal the depth of highly coupled complexes within the class II/III region. From this study, complex $\mathbf{4}^-$ displays temperature independence in intervalence band energies in optical electron transfer as well as temperature independence in IR ν(CO) band shape, which points to the lack of solvent dynamic contribution to the nuclear coordinate. The lack of dependence on solvent dynamics of a class II mixed valence system sets it apart from a borderline class II/III mixed valence system. As a mixed valence system enters the "early" borderline class II/III regime, the influence of dynamic contributions from the solvent becomes evident. Vibrational and optical investigations of $\mathbf{3}^-$ and $\mathbf{2}^-$ reveal solvent dependence of the mixed valence character. In particular, we found that restricting solvent motion (by lowering the temperature) favors delocalized behavior. As mixed valence systems transition through the later end of borderline class II/III to class III, solvent and temperature dependence of electron transfer begin to wane, as in $\mathbf{1}^-$. This is a result of solvent dynamics becoming nearly decoupled from electron transfer as the rate of ET becomes faster than solvent response. This study of mixed valence ions $\mathbf{1}^-$—$\mathbf{4}^-$ has provided a clearer understanding of the borderline of delocalization. It has provided guidelines for establishing where a particular system lies within the border, and criteria that apply to "late" class II, class II/III borderline, "late" borderline, and class III that we believe can be applied more widely.

ASSOCIATED CONTENT

Supporting Information. Temperature-dependent infrared spectra of $\mathbf{4}^-$ in acetonitrile, curve fits for spectra in Figure 2, integrated band intensities and exctinction coefficients for complexes $\mathbf{1}^-$—$\mathbf{4}^-$, and details of determination of ΔG_{ac}. This material is available free of charge via the Internet at http://pubs.acs.org.

AUTHOR INFORMATION

Corresponding Author
ckubiak@ucsd.edu

ACKNOWLEDGMENT

The authors thank Mr. Mark Llorente for the code used in Matlab simulations and Dr. John Goeltz and Mr. Gabriele Canzi for assistance with DFT calculations. We also thank Professor Michael Tauber and his research group for use of their Shimadzu UV 3600 while ours was out overlong for repairs. This work was supported by the National Science Foundation under Grant CHE-0616279.

REFERENCES

(1) Creutz, C.; Taube, H. *J. Am. Chem. Soc.* **1969**, *91*, 3988.
(2) Hush, N. S. *Prog. Inorg. Chem.* **1967**, *8*, 391.
(3) Robin, M. B.; Day, P. *Adv. Inorg. Chem. Radiochem.* **1967**, *10*, 247.
(4) Brunschwig, B. S.; Sutin, N. *Coord. Chem. Rev.* **1999**, *187*, 233.
(5) Chisholm, M. H. *Proc. Natl. Acad. Sci. USA* **2007**, *104*, 2563.
(6) Demadis, K. D.; Hartshorn, C. M.; Meyer, T. J. *Chem. Rev.* **2001**, *101*, 2655.
(7) Oh, D. H.; Sano, M.; Boxer, S. G. *J. Am. Chem. Soc.* **1991**, *113*, 6880.
(8) Reimers, J. R.; Hush, N. S. *Chem. Phys.* **1996**, *208*, 177.
(9) Ondrechen, M. J.; Ko, J.; Zhang, L. T. *J. Am. Chem. Soc.* **1987**, *109*, 1672.

(10) D'alessandro, D. M.; Topley, A. C.; Davies, M. S.; Keene, F. R. *Chem.—Eur. J.* **2006**, *12*, 4873.
(11) Petrov, V.; Hupp, J. T.; Mottley, C.; Mann, L. C. *J. Am. Chem. Soc.* **1994**, *116*, 2171.
(12) Hupp, J. T.; Dong, Y. H. *Inorg. Chem.* **1994**, *33*, 4421.
(13) Brunschwig, B. S.; Creutz, C.; Sutin, N. *Chem. Soc. Rev.* **2002**, *31*, 168.
(14) Glover, S. D.; Goeltz, J. C.; Lear, B. J.; Kubiak, C. P. *Eur. J. Inorg. Chem.* **2009**, 585.
(15) D'Alessandro, D. M.; Keene, F. R. *Chem. Soc. Rev.* **2006**, *35*, 424.
(16) Lear, B. J.; Glover, S. D.; Salsman, J. C.; Londergan, C. H.; Kubiak, C. P. *J. Am. Chem. Soc.* **2007**, *129*, 12772.
(17) Salsman, J. C.; Ronco, S.; Londergan, C. H.; Kubiak, C. P. *Inorg. Chem.* **2006**, *45*, 547.
(18) Ito, T.; Hamaguchi, T.; Nagino, H.; Yamaguchi, T.; Washington, J.; Kubiak, C. P. *Science* **1997**, *277*, 660.
(19) Ito, T.; Hamaguchi, T.; Nagino, H.; Yamaguchi, T.; Kido, H.; Zavarine, I. S.; Richmond, T.; Washington, J.; Kubiak, C. P. *J. Am. Chem. Soc.* **1999**, *121*, 4625.
(20) Sutin, N. In *Electron Transfer-from Isolated Molecules to Biomolecules*; Jortner, J., Bixon, M., Eds.; Advances in Chemical Physics, Vol. 106; J. Wiley: New York, 1999; Part 1, p 7.
(21) Londergan, C. H.; Salsman, J. C.; Ronco, S.; Dolkas, L. M.; Kubiak, C. P. *J. Am. Chem. Soc.* **2002**, *124*, 6236.
(22) Horng, M. L.; Gardecki, J. A.; Papazyan, A.; Maroncelli, M. *J. Phys. Chem.* **1995**, *99*, 17311.
(23) Chen, P.; Meyer, T. J. *Inorg. Chem.* **1996**, *35*, 5520.
(24) Glover, S. D.; Goeltz, J. C.; Lear, B. J.; Kubiak, C. P. *Coord. Chem. Rev.* **2010**, *254*, 331.
(25) Jaguar 3.5; Schrodinger, Portland, OR, 1998.
(26) Hay, P. J.; Wadt, W. R. *J. Chem. Phys.* **1985**, *82*, 299.
(27) Zhang, L. T.; Ko, J. J.; Ondrechen, M. J. *J. Phys. Chem.* **1989**, *93*, 3030.
(28) Ferretti, A.; Lami, A.; Ondrechen, M. J.; Villani, G. *J. Phys. Chem.* **1995**, *99*, 10484.
(29) Londergan, C. H.; Kubiak, C. P. *J. Phys. Chem. A.* **2003**, *107*, 9301.
(30) Sutin, N. J. *Prog. Inorg. Chem.* **1983**, *30*, 441.
(31) Crutchley, R. J. *Adv. Inorg. Chem.* **1994**, *41*, 273.
(32) Grozema, F. C.; Berlin, Y. A.; Siebbeles, L. D. A.; Ratner, M. A. *J. Phys. Chem. B* **2010**, *114*, 14564.
(33) Kurnikov, I. V.; Tong, G. S. M.; Madrid, M.; Beratan, D. N. *J. Phys. Chem. B* **2002**, *106*, 7.
(34) Lewis, F. D.; Wu, Y. S.; Zhang, L. G.; Zuo, X. B.; Hayes, R. T.; Wasielewski, M. R. *J. Am. Chem. Soc.* **2004**, *126*, 8206.
(35) Reimers, J. R.; Hush, N. S. *Chem. Phys.* **1993**, *176*, 407.
(36) Blackburn, J. L.; Selmarten, D. C.; Ellingson, R. J.; Jones, M.; Micic, O.; Nozik, A. J. *J. Phys. Chem. B* **2005**, *109*, 2625.
(37) Cai, X. C.; De, P. K.; Anyaogu, K. C.; Adhikari, R. M.; Palayangoda, S. S.; Neckers, D. C. *Chem. Commun.* **2009**, 1694.
(38) Lear, B. J.; Chisholm, M. H. *Inorg. Chem.* **2009**, *48*, 10954.
(39) Glover, S. D.; Lear, B. J.; Salsman, C.; Londergan, C. H.; Kubiak, C. P. *Philos. Trans. R. Soc., A* **2008**, *366*, 177.
(40) Londergan, C. H.; Rocha, R. C.; Brown, M. G.; Shreve, A. P.; Kubiak, C. P. *J. Am. Chem. Soc.* **2003**, *125*, 13912.
(41) Rocha, R. C.; Brown, M. G.; Londergan, C. H.; Salsman, J. C.; Kubiak, C. P.; Shreve, A. P. *J. Phys. Chem. A* **2005**, *109*, 9006.
(42) Londergan, C. H.; Salsman, J. C.; Lear, B. J.; Kubiak, C. P. *Chem. Phys.* **2006**, *324*, 57.
(43) Kumar, K.; Kurnikov, I. V.; Beratan, D. N.; Waldeck, D. H.; Zimmt, M. B. *J. Phys. Chem. A* **1998**, *102*, 5529.
(44) Hush, N. S. *Electrochim. Acta* **1968**, *13*, 1005.
(45) Vath, P.; Zimmt, M. B.; Matyushov, D. V.; Voth, G. A. *J. Phys. Chem. B* **1999**, *103*, 9130.
(46) Pekar, S. *Zh. Eksp. Teor. Fiz.* **1946**, *16*, 341.
(47) Simon, J. D. *Acc. Chem. Res.* **1988**, *21*, 128.
(48) Weaver, M. J. *Chem. Rev.* **1992**, *92*, 463.
(49) Lambert, C.; Noll, G.; Schelter, J. *Nat. Mater.* **2002**, *1*, 69.
(50) Launay, J.-P.; Coudret, C.; Hortholary, C. *J. Phys. Chem. B* **2007**, *111*, 6788.